International Journal of Gas Turbine, Propulsion and Power Systems
June 2024, Volume 15, Number 3

Cooling Model Calibration in a Collaborative Turbine Preliminary Design Process Using the NASA Energy Efficient Engine Part II: 1D Turbine Modeling

Francisco Carvalho[1], Patrick Wehrel[2], Clemens Grunwitz[1], Robin Schöffler[1], Robin G. Brakmann[1]

[1] German Aerospace Center (DLR), Institute of Propulsion Technology, Turbine Department, Göttingen, Germany
[2]German Aerospace Center (DLR), Institute of Propulsion Technology, Engine Department, Cologne, Germany

ABSTRACT

Accurately estimating turbine cooling requirements at a preliminary design stage is crucial for modeling the overall propulsive system. The operating conditions of compressor, combustor and turbine are significantly influenced by these requirements. Empirical cooling models have thus far provided reliable initial estimations. For next-generation aero-engines this solution becomes inadequate. To address this challenge, an alternative semi-empirical approach based on an established cooling model is built into a collaborative turbine design tool chain. This cooling model is applied to the two cooled high-pressure turbines developed by P&W and GE within the NASA E^3 program for both validation and to provide calibrated model parameters for future studies. Finally, sensitivity analysis provide a better understanding on how cooling requirements can be reduced through turbine preliminary design decisions, material and cooling technologies. This work focuses on 1D turbine studies with an accompanying paper on 0D engine modeling.

NOMENCLATURE

A	Area
Bi	Biot number
c	Blade chord
F_{sa}	Correction factor
K	Correlation parameter, cooling flow factor
h	Heat transfer coefficient
c_p	Isobaric heat capacity
Ψ	Loading coefficient
$\dot{m}$	Mass flow
AN^2	Mechanical load parameter
Nu	Nusselt number
s	Pitch
p	Pressure
Pr	Prandtl number
R	Reaction
Re	Reynolds number
St	Stanton number
T	Temperature
l	Thickness
ε_f	Adiabatic film cooling effectiveness
Θ	Arbitrary variable
β_1	Blade inlet angle
β_2	Blade outlet angle
η_c^*	Combined cooling efficiency
η_c	Cooling efficiency
ε_0	Cooling effectiveness
ϕ	Flow coefficient
Π	Pressure ratio
σ	Solidity
λ	Thermal conductivity
η_{Ts}	Turbine isentropic efficiency

Subscripts

aw	Adiabatic wall
b	Base material
c	Coolant
g	Gas
i	Inlet
o	Outlet
rel	Relative
s	Surface
t	Total

Abbreviations

ADP	Aerodynamic design point
CDP	Cooling design point
E3	Energy Efficient Engine
HLP	Heat load parameter
HPT	High-pressure turbine
IF	Interpolation factor
SF	Scaling factor

Manuscript Received on July 31, 2023
Review Completed on December 5, 2023

INTRODUCTION

Decisions made at a preliminary turbine design stage can significantly affect cooling requirements and the overall thermodynamic cycle. In the absence of detailed information on the airfoil geometry and the internal cooling design, estimating these requirements becomes a challenge. Thus far, the 1D turbine pre-design tool `PrEDiCT` [1], combined with empirical data [2], provided reliable initial estimations for cooling requirements. For next generation aero-engines, operating conditions may significantly change. With higher turbine inlet temperatures as well as new materials and cooling technologies, this empirical data becomes inadequate. To address this challenge, a semi-empirical approach is built into `PrEDiCT`. This updated approach is based on the well established *Holland and Thake* cooling model [3], already extensively adopted in the literature (e.g. [4, 5]). Nonetheless, calibrated values for various parameters of this cooling model related to the airfoil geometry, heat transfer and cooling technology are rarely published. To address this void, the cooling model is applied to two cooled high-pressure turbines developed by P&W and GE within the NASA Energy Efficient Engine (E^3) program [6, 7]. The result-

Copyright ©2024 Francisco Carvalho, Patrick Wehrel, Clemens Grunwitz, Robin Schöffler, Robin G. Brakmann

ing calibrated model parameter values serve both as input for future studies at turbine design level and to establish simplified cooling modeling methods for lower fidelity tools.

The work is divided in two parts. In Part I [8], the P&W and the GE engines are reconstructed with a 0D engine modeling tool. This reconstruction is based on the information published in the manufacturers' reports (often in normalized quantities) and is essential to obtain a complete set of operating requirements for the turbine modeling. This output is used in Part II (the current paper) to generate both P&W and GE HPTs with a 1D turbine modeling tool. A special focus is set on the reconstruction of cooling system and on the calibration of the cooling model (as already mentioned). Finally, the turbine models generated in Part II are used in Part I for a coupled 0D engine - 1D turbine modeling analysis. This first coupled approach is compared to a second approach with a simplified cooling model, also based on the output from Part II.

The generated turbine models themselves are a valuable source not only for lower fidelity tools (as demonstrated with Part I), but also for more accurate cooling design methods such as PICCOOLO [9], which resolves the airfoil profile geometry, internal cooling and film cooling. This enables the design and detailed evaluation of cooling systems for turbine vanes and blades, requiring input on the flow and fluid state both at the row inlet and outlet.

With a validated cooling model, sensitivity studies at turbine level provide a better understanding on how cooling requirements can be reduced through turbine preliminary design decisions as well as material and cooling technologies.

METHODS

TURBINE MODELING IN PrEDiCT

The 1D meanline program PrEDiCT is directed at generating a preliminary design of a multi-spool turbine as part of a holistic design process chain introduced in [10]. As the first step in the tool chain, minimal input is required: power requirements, shaft speed, and inlet mass flow. From the provided engine operating range, two operating points are selected at this stage. Firstly, an aerodynamic design point ADP for which the turbine geometry and efficiency are optimized and secondly, a cooling design point CDP for which the cooling system is dimensioned. The current study focuses heavily on the latter. The relative cooling requirements estimated for CDP are assumed constant between both operating points. With this, PrEDiCT calculates stage number and characteristics along with the annulus contour to meet the target power delivery at ADP. Parameters such as reaction, flow coefficient or Zweifel number can be adjusted by the user in an iterative process to tune the turbine geometry. Aerodynamic profile, secondary and tip losses are estimated through loss correlations from *Ainley and Mathieson* [11], *Dunham and Came* [12], *Kacker and Okapuu* [13] and *Benner and Sjolander* [14]. Ultimately, the tool delivers meanline thermodynamic quantities of the flow and cooling requirements at each row. In addition to the meanline characterization, radial flow variations are also described through a variable twist law. The reader is referred to [1] for detailed information.

COOLING MODELING IN PrEDiCT

The introduced cooling model is based on the assumption from Eq. 1. Energy is transferred from the mainstream flow to the coolant flow through an airfoil with infinite thermal conductivity and thus uniform temperature [3, 4]. From this, Eq. 2 is derived to obtain the airfoil coolant mass flow relative to the row inlet mass flow.

$$\int_0^{A_s} h_g \cdot (T_{t,aw} - T_b) \cdot dA_s = \dot{m}_c \cdot c_{p,c} \cdot (T_{t,c,o} - T_{t,c,i}) \tag{1}$$

$$\dot{m}_{c,rel} = \frac{c_{p,g}}{c_{p,c}} \cdot \frac{A_s}{A_g} \cdot St_g \cdot \frac{T_{t,aw} - T_b}{T_{t,c,o} - T_{t,c,i}} \tag{2}$$

In Eq. 2, the ratio between mainstream flow and coolant flow specific heat capacities is given by $c_{p,g}/c_{p,c}$. The A_s/A_g is the ratio between airfoil surface area and mainstream flow cross-sectional area at the throat. The mainstream flow Stanton number St_g models

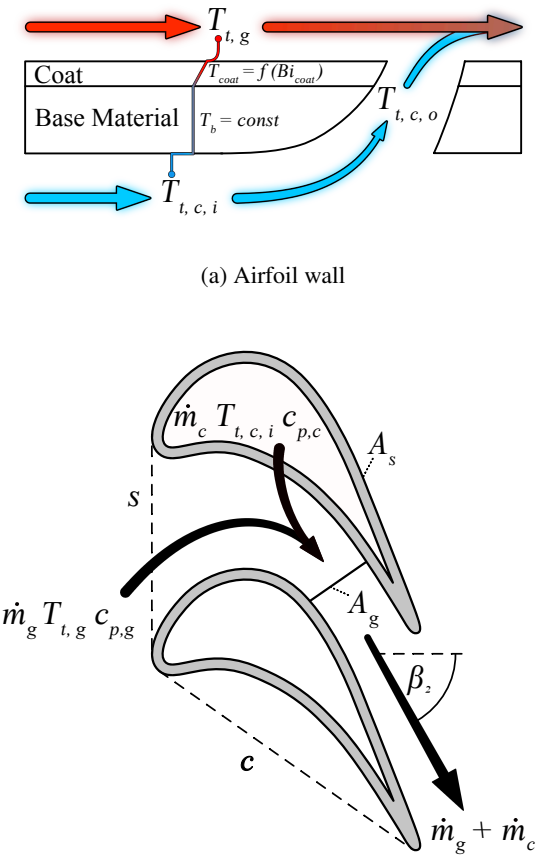

(a) Airfoil wall

(b) Row

Fig.1: Diagram and notation for the heat transfer model

the heat transfer to the airfoil and the final term must be rearranged into the heat load parameter *HLP*. Each of the listed parameters is briefly elaborated below.

The ratio A_s/A_g is estimated in a 2D plane through the airfoil perimeter and the throat width, as depicted in Fig. 1b. The throat width is a function of pitch s and the outlet angle β_2 [15]. The airfoil perimeter is at least twice the chord length $2 \cdot c$ and varies with deflection and airfoil thickness. The parameter F_{sa} reflects this influence and acts as a correction factor [16]. This results in the definition from Eq. 3. For the current study, A_s/A_g is calculated at five radial stations before being averaged.

$$\frac{A_s}{A_g} = \frac{2 \cdot c \cdot F_{sa}}{s \cdot \cos \beta_2} \tag{3}$$

Both the adiabatic wall temperature T_{aw} and the cooling air temperature at the airfoil outlet $T_{t,c,o}$ are challenging to determine at this fidelity level. To bypass this problem, the last term of Eq. 2 is transformed to define the *HLP* as a function of internal cooling efficiency η_c, adiabatic film cooling effectiveness ε_f and cooling effectiveness ε_0. Applying Eq. 5, Eq. 6 and Eq. 7, leads to the *HLP* definition from Eq. 4. In the presence of a protective coating, the *HLP* is modified through the coating Biot number Bi_{coat} [4]. The Bi_{coat}, defined in Eq. 8, is a function of the heat transfer coefficient between mainstream flow and coating surface h_g, coating thickness l_{coat} and thermal conductivity λ_{coat}.

Ultimately, the *HLP* is a dimensionless representation of the coolant mass flow defined by the airfoil cooling technology level through η_c and ε_f. The cooling efficiency models the heating of the cooling air inside the airfoil and the film cooling effectiveness the effect of the protective film [3]. Both are a function of the averaged

mainstream flow inlet temperature $T_{t,g}$, the coolant air inlet $T_{t,c,i}$ and outlet $T_{t,c,o}$ temperature and the airfoil base material maximum allowable temperature T_b shown in Fig. 1. In the absence of higher fidelity data from PICCOOLO, η_c and ε_f are a user-input, turning this into a semi-empirical approach. Calibrated values for these two parameters are discussed in the results section and serve as input for a first iteration in future turbine design efforts.

$$HLP = \frac{\varepsilon_f \cdot (1-\eta_c) + \varepsilon_0 \cdot (\varepsilon_f \cdot \eta_c - 1)}{\eta_c \cdot (\varepsilon_0 - 1)} \cdot \frac{1}{1+Bi_{coat}} \tag{4}$$

$$\eta_c = \frac{T_{t,c,o} - T_{t,c,i}}{T_b - T_{t,c,i}} \tag{5}$$

$$\varepsilon_f = \frac{T_{t,g} - T_{t,aw}}{T_{t,g} - T_{t,c,o}} \tag{6}$$

$$\varepsilon_0 = \frac{T_{t,g} - T_b}{T_{t,g} - T_{t,c,i}} \tag{7}$$

$$Bi_{coat} = \frac{h_g \cdot l_{coat}}{\lambda_{coat}} \tag{8}$$

Moreover, η_c and ε_f can be represented through a combined cooling efficiency η_c^*, defined in Eq. 9.

$$\eta_c^* = \frac{1}{HLP} \cdot \left(\frac{\varepsilon_f + (HLP \cdot (1+Bi_{coat}) - \varepsilon_f) \cdot \eta_c}{1-\varepsilon_f} \right) \tag{9}$$

The averaged Stanton number St_g through the airfoil can be approximated with Eq. 10 by assuming a K value between $0.285 - 0.5$ [1, 5, 17]. This dispenses with the need for information on the averaged mainstream flow Nusselt number Nu_g and on the heat transfer coefficient h_g. In the current implementation of the cooling model however, the Nu_g is estimated from the row outlet Reynolds number $Re_{g,o}$ using empirical data from *Louis* [18], yielding directly St_g and h_g. The Prandtl number Pr_g is assumed constant at 0.7.

$$St_g = \frac{Nu_g}{Re_g \cdot Pr_g} \approx K \cdot Re_g^{-0.37} \cdot Pr_g^{-2/3} \tag{10}$$

Given that the experimental data from *Louis* provides a Nu_g range for any $Re_{g,o}$ value, an upper and a lower limit are determined. The final Nu_g is calculated by means of an interpolation factor IF, see Eq. 11.

$$Nu_{g,L} = 0.5449 \cdot Re_{g,o}^{0,5156} \tag{11a}$$

$$Nu_{g,U} = 0.0525 \cdot Re_{g,o}^{0,7509} \tag{11b}$$

$$Nu_g = Nu_{g,L} + IF \cdot (Nu_{g,U} - Nu_{g,L}) \tag{11c}$$

From the Nusselt number Nu_g, the heat transfer coefficient h_g is calculated as in Eq. 12. If higher fidelity data is available, IF can be adjusted to calibrate Nu_g, h_g and ultimately St_g. This calibration is discussed in the results section for both turbines.

$$h_g = \frac{Nu_g \cdot \lambda_g}{c} \tag{12}$$

The cooling model discussed thus far only estimates the cooling requirements for the airfoil $\dot{m}_{c,rel}$. However, in addition to the airfoil itself, platform or disc cooling may also be required for a particular row. This overall cooling mass flow is represented by $\dot{m}_{c,rel,row}$. If the goal is to estimate $\dot{m}_{c,rel,row}$, Eq 2 may be multiplied by the scaling factor SF from Eq. 13. Based on the literature, values for this scaling factor are calculated and provided in the results section for each P&W and GE HPT row.

$$SF = \frac{\dot{m}_{c,rel,row}}{\dot{m}_{c,rel}} \tag{13}$$

Note that the implementation of this model in PrEDiCT is limited to averaged quantities. Specifically, $T_{t,g}$ and $c_{p,g}$ are mass averaged over the row inlet plane and $T_{t,c,i}$ and $c_{p,c}$ are mass averaged over the various secondary air system feeding channels to the airfoil. Also, St_g, h_g and T_b are averaged over the entire airfoil. Aspects such as mainstream flow temperature profiles or material temperature distributions are not modeled.

NASA E^3 TURBINE MODELING

The Energy Efficiency Engine (E^3) program was conducted under parallel National Aeronautics and Space Administration (NASA) contracts by Pratt & Whitney (P&W) and the General Electric Company (GE). The E^3 program was created to develop fuel saving technology for future transport engines through new aerodynamic, mechanic and system technologies.

Both manufacturers provide detailed reporting at system and component design level [6, 7]. The published data includes turbine aerodynamic analysis as well as structural mechanical and thermal management analysis for the cooled turbine airfoils. While this does provide valuable validation data for select studies, it occasionally lacks information on essential parameters to model the high-pressure turbines (HPT) and their cooling systems. To address this problem and generate a complete input dataset, both cooled high-pressure turbines are modeled in a collaborative process between engine and turbine level within GTlab [19], a framework for multidisciplinary design of turbo-machine systems. Some aspects of the modeling process are provided below. For additional information, the reader is referred to [8].

The P&W HPT is designed for cruise conditions, which is set as the ADP. The manufacturers design report and Part I [7, 8] are the main sources for modeling in PrEDiCT. GE's HPT is optimised for maximum climb conditions (also set as the ADP) and is modeled in PrEDiCT according to the data provided in [6, 8]. The P&W HPT is designed for a power requirement of 14.1 MW with a shaft-speed of 220.5 1/s at ADP. The GE HPT is designed for 16.03 MW at 210.8 1/s at ADP. In both cases, there is a good agreement between the literature and the modeled high-pressure turbines, depicted in Fig.2. Tab. 1 lists selected output data from PrEDiCT for the modeled turbines, along with a deviation to the data collected from the literature. In particular, stage parameters such as loading Ψ, flow coefficient ϕ, reaction R and pressure ratio Π largely match the literature, assuring a similarity between turbines. Modeled isentropic efficiency η_{Ts} values are also listed. In PrEDiCT, η_{Ts} is defined according to [20, p. 670]. It is unclear how η_{Ts} is calculated in the literature and a direct comparison is not advisable.

The cooling system is the main focus of the current study. To be able to compare the output of the cooling model between the two HPTs, the CDP is set to takeoff for both turbines. P&W does provide data for takeoff conditions, but GE only provides data for end-of-field conditions. The missing data for GE at takeoff is obtained from [8], where both engines are modeled in design and off-design. This includes parameters such as relative coolant mass flow, material temperature as well as thermodynamic conditions of mainstream and coolant flow. The design reports provide cooling requirement data relative to the compressor inlet mass flow, $\dot{m}_c/\dot{m}_{ref}$. This is converted in [8] to values relative to the row inlet mass flow, $\dot{m}_c/\dot{m}_g$ for compatibility with the cooling model. Additionally, the distinction is made between airfoil and overall row coolant mass flow to estimate the scaling factor SF from Eq. 13. Mass flow and scaling factor values are provided in Tab. 3 for each row. Finally, coolant and mainstream flow averaged temperature and pressure data is available, but airfoil base material temperature is provided in the literature only in peak values. While this is relevant at a later design stage, it does not fit this initial averaged approach. For the P&W HPT, the cooling effectiveness ε_0 is kept constant between peak conditions and averaged conditions at CDP to estimate T_b. Peak values are not available for GE's HPT at CDP. As a result, the cooling effectiveness is calculated for $T_{t,c,i}$, $T_{t,g,peak}$ and $T_{b,peak}$ based on the literature data at end-of-field and kept constant to estimate T_b at CDP. The resulting output is listed in Tab. 2. For the GE rows, $T_{t,c,i}$ is given for both end-of-field conditions and for

Table 1: Output from PrEDiCT for NASA E^3 HPTs at ADP with relative deviation from literature data [6, 7, 8]

Component		Ψ [−]	ϕ [−]	Π [−]	R [−]	AN^2 [$m^2/min^2/1E7$]	σ_{stator} [−]	σ_{rotor} [−]	η_{Ts} [−]
P&W	Spool 1	1.67 (3.1%)	0.35 (0.0%)	4.00 (0.0%)	0.43 (0.0%)	2.58 (-1.5%)	0.44 (-)	0.76 (-)	0.885
GE	Stage 1	1.43 (-3.4%)	0.50 (-)	2.25 (0.0%)	0.34 (0.0%)	1.29 (-)	0.74 (4.2%)	1.02 (6.3%)	0.911
	Stage 2	1.09 (-2.7%)	0.53 (-)	2.11 (0.0%)	0.33 (0.0%)	2.32 (-)	1.08 (0.9%)	1.01 (-4.7%)	0.907
	Spool 1	-	-	4.75 (0.0%)	-	-	-	-	0.901

Table 2: Calculation of averaged airfoil base material temperature T_b at CDP for NASA E^3

Component		$T_{t,c,i}$ [K]	$T_{t,g,peak}$ [K]	$T_{b,peak}$ [K]	ε_0 [−]	$T_{t,g}$ [K]	T_b [K]	Source
P&W	S1	850.2	2161.2	1353.0	0.617	1708.2	1179.2	[7, pp. 30, 37]
	R1	829.2	1698.2	1263.5	0.500	1416.0	1122.5	[7, pp. 40, 44]
GE	S1	883.2 / 861.2	2012.2	1279.2	0.649	1698.3	1154.9	[8], [6, pp. 27, 29, 33]
	R1	855.2 / 833.2	1669.2	1302.7	0.450	1461.7	1178.8	[8], [6, p. 47]
	S2	761.2 / 738.5	1463.2	1287.5	0.250	1332.8	1184.1	[8], [6, p. 55]
	R2	866.2 / 844.0	1311.2	1227.5	0.188	1196.0	1129.9	[8], [6, pp. 54, 58]

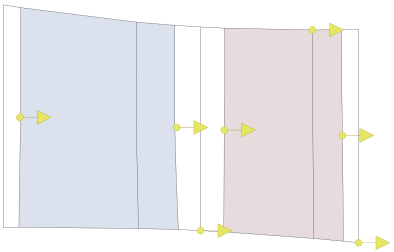

(a) P&W

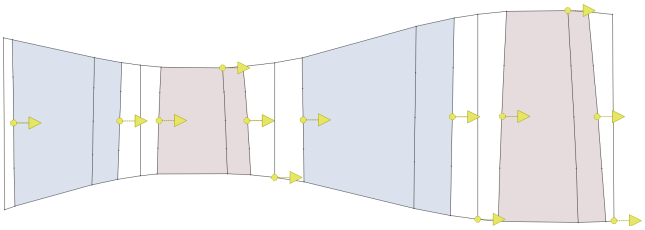

(b) GE

Fig.2: High-pressure turbine flow path generated in PrEDiCT

CDP (takeoff), in this order. On a final note, all airfoils are coated only with a high thermal conductivity Ni-based oxidation resistant coating. Its thermal effect is therefore considered negligible and the coating Biot number $Biot_{coat}$ is set to zero.

Table 3: Mass flow per row at ADP and scaling factor SF for NASA E^3 HPTs [6, 7, 8]

Component		$\dot{m}_i$ [kg/s]	$\dot{m}_o$ [kg/s]	SF [−]
P&W	S1	27.30	30.00	1.35
	R1	30.00	31.62	1.88
GE	S1	26.26	29.31	1.53
	R1	29.31	31.24	1.85
	S2	31.24	31.66	1.23
	R2	31.66	32.22	2.32

RESULTS AND DISCUSSION

The parameters from Eq. 2 and Eq. 4 have been calculated or calibrated to match the $\dot{m}_{c,rel}$ values from the manufacturers design reports and are discussed bellow.

Literature data on the ratio A_s/A_g is scarce. While [21, 22] estimate a ratio of $10-20$ for a generic airfoil, this is dependent on a series of geometrical parameters such as chord, stagger angle or pitch. With this in mind and using the geometrical data provided within PrEDiCT, this ratio is calculated and listed in Tab. 4. A large variation is perceived, in the range $12-21$ for stator rows and $5-11$ for rotor rows. Clearly, A_s/A_g tends to be higher for stator rows than for rotor rows by an averaged factor of ≈ 2. To estimate the airfoil surface area A_s, the correction parameter F_{sa} is calculated from the meanline profiles provided by the design reports. This correction parameter appears to be correlated with the flow deflection $|\beta_1-\beta_2|$ and the airfoil maximum thickness to chord ratio t_{max}/c, here represented by the parameter $S=|\beta_1-\beta_2|\cdot t_{max}/c$. This dependency should be analysed for a larger dataset and can prove useful to estimate airfoil surface area at a pre-design stage.

Table 4: Airfoil geometric characteristics for NASA E^3 HPTs

Component		S [rad]	F_{sa} [−]	A_s/A_g [−]	Source
P&W	S1	0.26	1.13	21.1	[7, p. 13]
	R1	0.63	1.32	11.1	[7, p. 17]
GE	S1	0.22	1.13	11.9	[6, p. 14]
	R1	0.39	1.29	7.1	[6, p. 14]
	S2	0.22	1.19	14.0	[6, p. 14]
	R2	0.27	1.12	5.1	[6, p. 14]

The internal cooling efficiency η_c and the film cooling effectiveness ε_f are input parameters for the cooling model. In the presence of film cooling, ε_f is kept constant while η_c is calibrated. This is the case for the first stage of both HPTs. The range for ε_f is set between $0.15-0.30$. GE's second stage is not film cooled and $\varepsilon_f=0$. Calibrated data are provided in Fig. 3. In particular, the high η_c in GE's second stage stator S2 is notable. Impingement cooling covers the complete inner surface of the GE S2 wall, resulting in a high internal heat transfer. Furthermore, in the absence of film cooling, the cooling air does not exit the airfoil in the vicinity of the impingement jet stagnation points. Instead, it must travel to the trailing edge and exit through the cooling holes at that position. Finally, the low thermal load for this airfoil leads to a low cooling mass flow requirement. Due to the high heat transfer, the longer travel route and the reduced cooling mass flow, the cooling air can absorb more heat. This contributes to an increased cooling mass flow exit temperature $T_{t,c,o}$ and ultimately to a higher η_c (see Eq. 5). While it is challenging to find comparative data in the literature, [3] provides cooling performance metrics for Rolls-Royce high-pressure turbine airfoils, some of which in the same range as the GE S2.

The corresponding heat load parameter HLP and cooling effectiveness ε_0 are depicted in Fig. 4. Both the P&W and the GE first

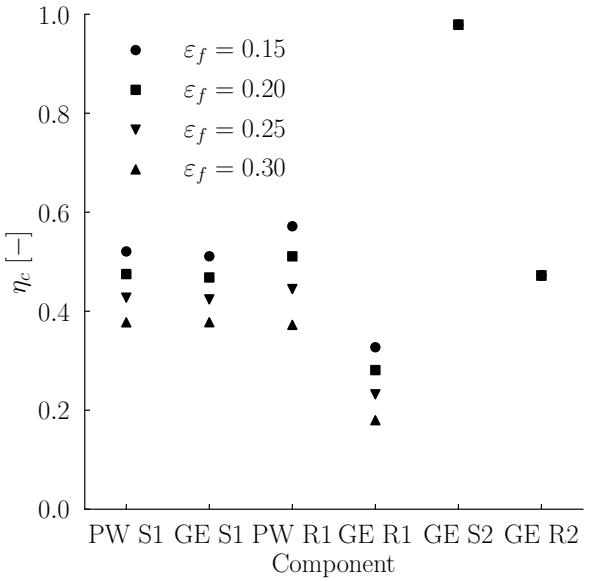

Fig.3: Calibrated cooling efficiency η_c at CDP for NASA E^3 HPTs

stage stators (S1) display similar *HLP* values, indicative of the similar cooling requirements. The same is true for both first stage rotors (R1). With the exception of GE's S2, all airfoils show a combined cooling efficiency η_c^* in the range $0.45 - 0.73$.

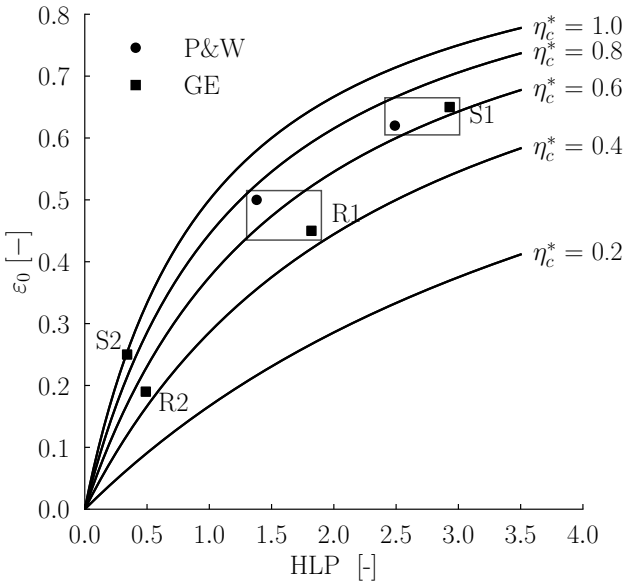

Fig.4: Cooling performance diagram at CDP for NASA E^3 HPTs

The Stanton number is reported in some studies to assume a value of $St_g \approx 0.005$ [22, 16]. *Torbidoni and Horlock* [5] resort instead to a correlation based on the experimental data from *Louis* [18]. The cooling model in this work uses the same experimental data to calculate the averaged Nusselt number Nu_g. The interpolation factor *IF* is adjusted to match the resulting averaged heat transfer coefficient h_g between `PrEDiCT` and the literature. The *IF* varies little for the P&W HPT, between 0.66 for the stator S1 and 0.70 for the rotor R1. In contrast to P&W, GE only provides data on the heat transfer coefficient for the first rotor R1. As a result, the interpolation factor, calibrated for GE R1, is assumed constant for all remaining GE airfoils. This ultimately means that the ratio between St_g and Re_g is kept constant throughout all GE airfoils, similar to approach from Eq. 10. The difference being that this ratio is calibrated a priori for GE's R1. Nevertheless, both solutions introduce a source of error that is not present in the modelling of P&W S1, P&W R1 and GE R1. A summary of the *IF* values along with the resulting h_g and St_g values are listed in Tab. 5 for both high-pressure turbines. For any one stage, variations in flow velocity and density lead to a lower row outlet Reynolds number $Re_{g,o}$ in the rotor, resulting in a consistently higher St_g than for the upstream stator, emphasizing the need for a flow dependent St_g estimation.

This flow dependent estimation of St_g is also key to understand how different operating conditions can affect the heat transfer to the airfoil and the cooling requirements. Turbine inlet conditions can change considerably throughout the operating range of an aircraft with a noticeable effect on both $Re_{g,o}$ and St_g. Fig. 5 depicts the sensitivity of the P&W stator St_g on the total row inlet pressure and temperature. A higher inlet pressure results in a higher fluid density and $Re_{g,o}$, leading to a lower St_g. Similarly, a higher inlet temperature leads to a higher St_g. Looking at this behaviour, the thermal load is expected to rise for operating points with a high inlet temperature and a low inlet pressure. Takeoff is typically selected as dimensioning point for the cooling system of civil aero-engines. In the presence of a wider operating range, as is the case of military aero-engines, high altitude operating points may exhibit an increased thermal load.

Table 5: Averaged heat transfer coefficient h_g and Stanton number St_g at CDP for NASA E^3 HPTs

Component		h_g $[W/m^2K]$	St_g $[10^{-3}]$	$IF[-]$	Source
P&W	S1	4734	1.25	0.70	[7, p. 37]
	R1	3492	1.72	0.66	[7, p. 44]
GE	S1	8114	1.94	1.16	-
	R1	6541	2.51	1.16	[6, p. 42]
	S2	4166	2.10	1.16	-
	R2	3465	2.85	1.16	-

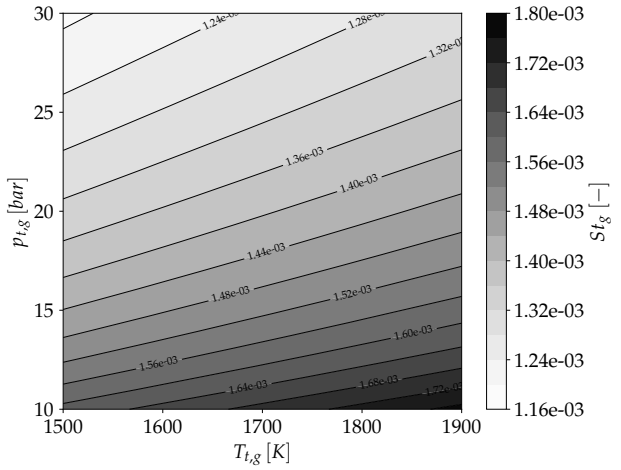

Fig.5: Sensitivity of averaged Stanton number St_g on row inlet conditions for NASA E^3 P&W HPT S1 calculated in `PrEDiCT`

Finally, a sensitivity analysis of cooling requirements on the cooling model input parameters (Θ) is briefly introduced in Fig. 6, again for the P&W HPT stator. In terms of new technologies, materials with higher maximum allowable temperatures (T_b) such as ceramic-matrix-composites [23, 24] should provide a remarkable

reduction in cooling requirements. This is followed by innovative internal cooling configurations (η_c) facilitated by additive manufacturing [25, 26], advancements in film cooling techniques (ε_f) and finally lower thermal conductivity coatings (Bi_{coat}).

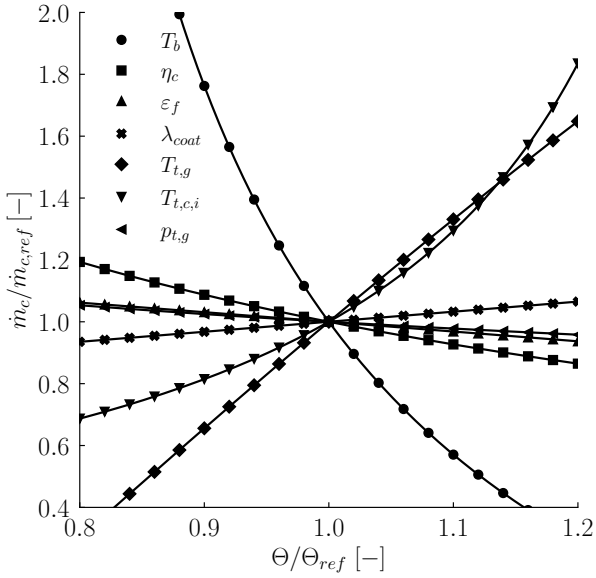

Fig.6: Sensitivity of coolant mass flow $\dot{m}_c$ on cooling model parameters for NASA E^3 P&W HPT S1 calculated in PrEDiCT

Looking again at Fig. 6, the total inlet temperature $T_{t,g}$ and coolant temperature $T_{t,c,i}$ significantly affect cooling requirements. Although the airfoil geometry (A_s/A_g) is not a directly iterable parameter to be listed in Fig. 6, it too has a significant effect on the cooling requirements. The potential for cooling reduction here may not come from new technologies, but instead from cooling oriented turbine pre-design decisions. In particular, both turbine geometry and flow conditions are heavily influenced at a pre-design stage by parameters such as reaction R and flow coefficient ϕ. Fig. 7 demonstrates the sensitivity of the P&W HPT cooling requirements on both these parameters. On all instances, the reference is set to the design values. A lower reaction results in a higher flow acceleration through the stator relative to the rotor. As a result, both rotor inlet absolute (c) and relative (v) inlet velocities increase, with $\Delta c > \Delta v$. Keeping in mind that

$$T_{t,g,abs} = T + \frac{c^2}{2 \cdot c_p}$$
$$T_{t,g,rel} = T + \frac{v^2}{2 \cdot c_p} \tag{14}$$

and that the static temperature T remains constant between coordinate systems, it is clear that

$$T_{t,g,abs} - T_{t,g,rel} = \frac{c^2 - v^2}{2 \cdot c_p} \tag{15}$$

Thus, a lower reaction leads to a lower $T_{t,g,rel}$ at the rotor inlet and finally to a reduction in cooling requirements. Furthermore, the flow coefficient ϕ largely controls the shape of the annulus geometry. For both stator and rotor in Fig. 7, increasing ϕ results in a lower A_s/A_g, leading to a further reduction in cooling. It is clear that both parameters (R and ϕ) alter the behaviour and performance of the turbine in design and off-design. Nevertheless, the tendencies shown highlight a valid approach for cooling reduction at a pre-design phase.

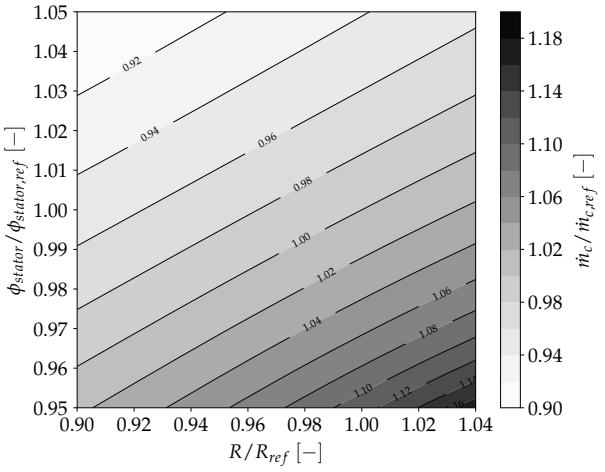

(a) Constant ϕ_{rotor}

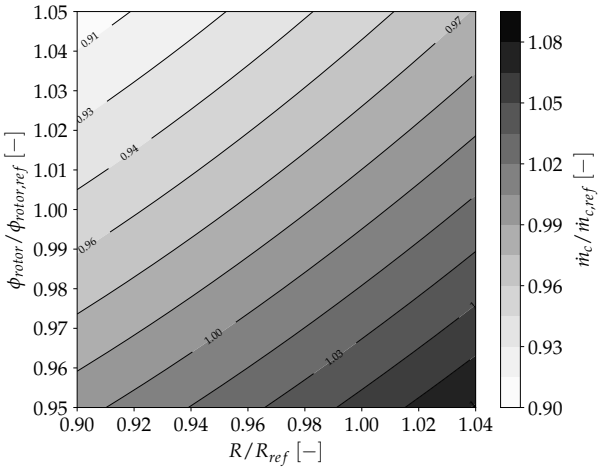

(b) Constant ϕ_{stator}

Fig.7: Sensitivity of the stage coolant mass flow $\dot{m}_c$ on stage reaction and flow coefficient for NASA E^3 P&W HPT calculated in PrEDiCT

The results discussed so far can also be used to facilitate the estimation of cooling requirements in lower fidelity tools. Looking at both Tab. 4 and Tab. 5, it becomes apparent that as the area ratio A_s/A_g decreases, the St_g tends to increase. In fact, the product of the two varies only between 0.023-0.026 for the first stage stators and 0.018-0.019 for the first stage rotors. Estimating both parameters requires information on turbine geometry and flow state that may not be accessible in lower fidelity tools. For such cases, the cooling model implemented in PrEDiCT can be simplified as in Eq. 16 with a constant $K = A_s/A_g \cdot St_g$. This approach is tested in [8] where a coupled 0D engine - 1D turbine modeling (using the turbine and the cooling models from this work) is compared to a 0D engine modeling with the simplified cooling model. The HPT inlet temperature T_g and the cooling flow temperature $T_{t,c,i}$ are varied independently by ±10%. Both modelling approaches deliver similar results. This demonstrates that Eq. 16 is a viable solution for 0D engine level studies, as long as calibrated K values are available (such as those provided in this work).

$$\dot{m}_{c,rel} = \frac{c_{p,g}}{c_{p,c}} \cdot K \cdot HLP \tag{16}$$

CONCLUSIONS

In the present work an established cooling model is implemented into a turbine preliminary design tool and calibrated for two cooled high-pressure turbines in a collaborative process between turbine (Part II) and engine performance modeling (Part I). The calibrated parameters are discussed and the implemented model is used for parametric analysis to provide insights on possible approaches to reduce cooling requirements.

In terms of new technologies, high temperature materials such as ceramic-matrix-composites appear to provide a significant potential for reducing cooling requirements. This is followed by innovative internal cooling configurations, improved film cooling techniques and enhanced thermal barrier coatings. Furthermore, the turbine geometry defined at a pre-design stage affects the flow state and the heat transfer to the airfoils. In particular, cooling requirements tend to decrease for lower stage reaction and higher flow coefficients. Considering these tendencies during turbine pre-design can help further reduce cooling requirements.

The averaged mainstream flow Stanton number is dependent on the row inlet temperature and pressure conditions. High altitude low pressure engine operating points can result in increased thermal loads. This should also be taken into account when dimensioning the turbine cooling requirements, especially for aero-engines with a wide operating range.

The estimated ratio between airfoil surface area and mainstream flow cross-sectional area ranges between $12-21$ for stators and $5-11$ for rotors. At the same time, the averaged mainstream flow Stanton number tends to be higher for rotors. In the end, the product of A_s/A_g with St_g varies only between 0.023-0.026 for the first stage stators and 0.018-0.019 for the first stage rotors. As a result, both could be replaced with a parameter $K = A_s/A_g \cdot St_g$ in a simplified cooling model for lower-fidelity design tools. Part I demonstrates the validity of this approach, as long as reliable calibrated values are provided (such as those provided in Part II).

In a first turbine design iteration, where output from PICCOOLO is not yet available, the cooling model becomes semi-empirical through the cooling efficiency and film cooling effectiveness. The current study provides empirical data on both parameters for a series of airfoils with different designs and operating conditions.

The points listed above serve as input for the pre-design of a next-generation turbine, planned for future work.

ACKNOWLEDGEMENTS

This work was supported by the DLR and executed within the projects ADAPT and Future Fighter Engine Technologies FFE+. We sincerely thank all project participants for their support.

REFERENCES

[1] Krumme, A. "Konzeption, Implementierung Und Anwendung Eines Automatisierten Aerothermodynamischen Vorentwurfsprozesses Fuer Axialturbinen". Universitaet Kassel, 2015.

[2] Grieb, H. *Projektierung von Turboflugtriebwerken*. Basel: Springer Basel, 2004. DOI: 10.1007/978-3-0348-7938-5.

[3] Holland, M. and Thake, T. "Rotor Blade Cooling in High Pressure Turbines". In: *Journal of Aircraft* 17.6 (1980), pp. 412–418. DOI: 10.2514/3.44668.

[4] Young, J. and Wilcock, R. "Modeling the Air-Cooled Gas Turbine: Part 2 - Coolant Flows and Losses". In: *Journal of Turbomachinery* 124.2 (2002), pp. 214–221. DOI: 10.1115/1.1415038.

[5] Torbidoni, L. and Horlock, J. "A New Method to Calculate the Coolant Requirements of a High-Temperature Gas Turbine Blade". In: *Journal of Turbomachinery* 127.1 (2005), pp. 191–199. DOI: 10.1115/1.1811100.

[6] Halila, E., Lenahan, D., and Thomas, T. *Energy Efficient Engine - High Pressure Turbine - Test Hardware Detailed Design Report*. CR-167955. NASA, 1982.

[7] Thulin, R., Howe, D., and Singer, I. *Energy Efficient Engine - High-Pressure Turbine Detailed Design Report*. CR-165608. NASA, 1982.

[8] Wehrel, P. and Carvalho, F. "Cooling Model Calibration in a Collaborative Turbine Preliminary Design Process Using the NASA Energy Efficient Engine Part I: 0D Performance Modeling". In: *International Journal of Gas Turbine, Propulsion and Power Systems* (2023).

[9] Schöffler, R., Grunwitz, C., and Brakmann, R. G. "A Semi-Empirical Model for Conceptual Turbine Vane Cooling Design and Optimization". In: *Proceedings of ASME Turbo Expo 2023*. ASME. Boston, USA, 2023.

[10] Grunwitz, C. et al. "A Comprehensive Multifidelity Design and Analysis Process for Cooled Axial Flow Turbines: From Concept to Component". In: *Proceedings of the International Gas Turbine Congress 2023*. IGTC. Kyoto, Japan, 2023.

[11] Ainley, D. G. and Mathieson, G. C. R. "A Method of Performance Estimation for Axial-Flow Turbines". In: *Aeronautical Research Council Reports and Memoranda* (1951).

[12] Dunham, J. and Came, P. M. "Improvements to the Ainley-Mathieson Method of Turbine Performance Prediction". In: *Journal of Engineering for Power* 92.3 (July 1, 1970), pp. 252–256. DOI: 10.1115/1.3445349.

[13] Kacker, S. C. and Okapuu, U. "A Mean Line Prediction Method for Axial Flow Turbine Efficiency". In: *Journal of Engineering for Power* 104.1 (Jan. 1, 1982), pp. 111–119. DOI: 10.1115/1.3227240.

[14] Benner, M. W., Sjolander, S. A., and Moustapha, S. H. "An Empirical Prediction Method For Secondary Losses In Turbines—Part II: A New Secondary Loss Correlation". In: *Journal of Turbomachinery* 128.2 (Apr. 1, 2006), pp. 281–291. DOI: 10.1115/1.2162594.

[15] Aungier, R. *Turbine Aerodynamics: Axial-Flow and Radial-Flow Turbine Design and Analysis*. New York: ASME Press, 2006. DOI: 10.1115/1.802418.

[16] Sanjay, Singh, O., and Prasad, B. "Influence of Different Means of Turbine Blade Cooling on the Thermodynamic Performance of Combined Cycle". In: *Applied Thermal Engineering* 28.17-18 (2008), pp. 2315–2326. DOI: 10.1016/j.applthermaleng.2008.01.022.

[17] Chiesa, P. and Macchi, E. "A Thermodynamic Analysis of Different Options to Break 60% Electric Efficiency in Combined Cycle Power Plants". In: *Journal of Engineering for Gas Turbines and Power* 126.4 (Oct. 1, 2004), pp. 770–785. DOI: 10.1115/1.1771684.

[18] Louis, J. "Systematic Studies of Heat Transfer and Film Cooling Effectiveness". In: *AGARD 229 - High Temperature Problems in Gas Turbine Engines*. 1977.

[19] Reitenbach, S. et al. "Collaborative Aircraft Engine Preliminary Design Using a Virtual Engine Platform, Part A: Architecture and Methodology". In: *AIAA Scitech 2020 Forum*. AIAA Scitech. Orlando, USA: American Institute of Aeronautics and Astronautics, 2020. DOI: 10.2514/6.2020-0867.

[20] Kurzke, J. and Halliwell, I. *Propulsion and Power: An Exploration of Gas Turbine Performance Modeling*. Springer, 2018.

[21] Horlock, J., Watson, D., and Jones, T. "Limitations on Gas Turbine Performance Imposed by Large Turbine Cooling Flows". In: *Journal of Engineering for Gas Turbines and Power* 123.3 (2001), pp. 487–494. DOI: 10.1115/1.1373398.

[22] Jonsson, M. et al. "Gas Turbine Cooling Model for Evaluation of Novel Cycles". In: *Proceedings of ECOS 2005*. ECOS. Trondheim, Norway, 2005.

[23] Wehrel, P. et al. “Performance and Emissions Benefits of Cooled Ceramic Matrix Composite Vanes for High Pressure Turbines”. In: *Proceedings of ASME Turbo Expo 2023*. ASME. Boston, USA, 2023.

[24] Zhu, D. *Aerospace Ceramic Materials: Thermal, Environmental Barrier Coatings and SiC/SiC Ceramic Matrix Composites for Turbine Engine Applications*. NASA/TM—2018-219884. NASA, 2018.

[25] Brakmann, R. G. et al. “A Numerical Analysis of Cross-Flow Reinforced Impingement Cooling with a U-Shaped Flow-Guide on the Hole Plate”. In: *Proceedings of ASME Turbo Expo 2023*. ASME. Boston, USA, 2023.

[26] Magerramova, L., Vasilyev, B., and Kinzburskiy, V. “Novel Designs of Turbine Blades for Additive Manufacturing”. In: *Proceedings of ASME Turbo Expo 2016*. ASME. Seoul, South Korea, 2016. DOI: 10.1115/GT2016-56084.

[27] Bisset, J. and Hower, D. *Energy Efficient Engine - Flight Propulsion System Preliminary Analysis and Design Report*. PWA-5594-248. NASA, 1983.

APPENDIX

Additional Nomenclature

α_g	Flow angle
P	Power
N	Shaft-speed

P&W HPT

Table 6: Comparison between PrEDiCT output and literature for the P&W HPT

Component		Parameter	Unit	PrEDiCT		Literature		Source
				ADP	CDP	ADP	CDP	
S1	Inlet	$T_{t,g}$	K	1633.0	1708.2	1633.0	1708.0	[7, p. 9]
		$p_{t,g}$	bar	13.24	29.62	13.24	29.62	[7, p. 9], [27, p. 40]
		$\dot{m}_g$	kg/s	27.30	-	27.30	-	[8]
		α_g	deg	0.00	-	0.00		[7, p. 12]
	Outlet	$T_{t,g}$	K	1558.0	1629.7	-	-	-
		$p_{t,g}$	bar	11.84	26.47	-	-	-
		$\dot{m}_g$	kg/s	30.00	-	30.00	-	[8]
		α_g	deg	79.59	-	79.70	-	[7, p. 12]
	SAS	$T_{t,c,in}$	K	760.3	850.2	760.3	850.2	[8], [7, p. 32]
		$p_{t,c,in}$	bar	13.56	30.35	13.56	-	[8]
		SF	-	1.35		1.35		[7]
R1	Inlet	$T_{t,g}$	K	1353.7	1416.0	-	-	-
		$T_{t,g,abs}$	K	1558.0	1629.7	1561.0	1641.0	[7, p. 9]
		$p_{t,g}$	bar	6.42	14.35	-	-	-
		$p_{t,g,abs}$	bar	11.84	26.47	-	-	-
		$\dot{m}_g$	kg/s	30.00	-	30.00	-	[8]
		α_g	deg	57.47	-	56.00	-	[7, p. 17]
	Outlet	$T_{t,g}$	K	1333.5	1394.8	-	-	-
		$T_{t,g,abs}$	K	1157.9	1211.2	-	-	
		$p_{t,g}$	bar	6.02	13.47	-	-	-
		$p_{t,g,abs}$	bar	3.31	7.40	3.30	-	[7, p. 9]
		$\dot{m}_g$	kg/s	31.62	-	31.62	-	[8]
		α_g	deg	-70.65	-	-73.20	-	[7, p. 17]
	SAS	$T_{t,c,in}$	K	738.8	829.2	738.8	829.2	[8], [7, p. 41]
		$p_{t,c,in}$	bar	7.93	17.76	7.93	-	[8]
		SF	-	1.88		1.88		[7]
Stage 1		P	MW	14.12	-	14.12	-	[8]
		N	1/s	220.50	-	220.50	-	[8]
		$\dot{m}_f$	kg/s	0.70	-	0.70	-	[8]
		Ψ	-	1.67	-	1.62	-	[7, p. 9]
		ϕ	-	0.35	-	0.35	-	[7, p. 9]
		Π	-	4.00	-	4.00	-	[7, p. 9]
		R	-	0.43	-	0.43	-	[7, p. 9]
		AN2	-	2.58	-	2.62	-	[7, p. 9]
		N. Stator Blades	-	24		24		[7, p. 13]
		N. Rotor Blades	-	54		54		[7, p. 17]
		Stator Solidity	-	0.44		-		-
		Rotor Solidity	-	0.76		-		
		η_{Ts}	-	0.885[4]	-	0.879[4]	-	[7, p. 9]

[4]Defined in PrEDiCT according to [20, p. 670]. Definition for cooled turbine isentropic efficiency is unclear from literature data.

GE HPT

Table 7: Comparison between PrEDiCT output and literature for the GE HPT

Component		Parameter	Unit	PrEDiCT		Literature		Source
				ADP	CDP	ADP	CDP	
S1	Inlet	$T_{t,g}$	K	1636.4	1698.3	1636.4	1698.3	[8]
		$p_{t,g}$	bar	13.21	31.19	13.21	31.19	[8]
		$\dot{m}_g$	kg/s	26.26	-	26.26	-	[8]
		α_g	deg	0.00	0.00	0.00	-	[6, p. 13]
	Outlet	$T_{t,g}$	K	1553.9	1612.7	-	-	-
		$p_{t,g}$	bar	12.71	30.99	-	-	-
		$\dot{m}_g$	kg/s	29.31	-	29.31	-	[8]
		α_g	deg	72.63	-	-	-	-
	SAS	$T_{t,c,in}$	K	808.6	861.2	808.6	861.2	[8]
		$p_{t,c,in}$	bar	13.54	31.97	13.54	31.97	[8]
		SF	-	1.53		1.53		[6]
R1	Inlet	$T_{t,g}$	K	1408.4	1461.7	-	-	-
		$T_{t,g,abs}$	K	1553.9	1612.7	-	-	-
		$p_{t,g}$	bar	8.26	19.50	-	-	-
		$p_{t,g,abs}$	bar	12.71	29.99	-	-	-
		$\dot{m}_g$	kg/s	29.31	-	29.21	-	[8]
		α_g	deg	41.05	-	-	-	-
	Outlet	$T_{t,g}$	K	1377.9	1430.0	-	-	-
		$T_{t,g,abs}$	K	1284.2	1332.8	-	-	-
		$p_{t,g}$	bar	7.98	18.83	-	-	-
		$p_{t,g,abs}$	bar	5.89	13.90	-	-	-
		$\dot{m}_g$	kg/s	31.24	-	31.24	-	[8]
		α_g	deg	-61.61	-	-	-	-
	SAS	$T_{t,c,in}$	K	780.2	833.2	780.2	833.2	[8]
		$p_{t,c,in}$	bar	13.91	32.83	13.91	32.83	[8]
		SF	-	1.85		1.85		[6]
S2	Inlet	$T_{t,g}$	K	1284.2	1332.8	-	-	-
		$p_{t,g}$	bar	5.89	13.90	-	-	-
		$\dot{m}_g$	kg/s	31.24	-	31.24	-	[8]
		α_g	deg	-5.46	-	-	-	
	Outlet	$T_{t,g}$	K	1276.5	1324.7	-	-	-
		$p_{t,g}$	bar	5.63	13.29	-	-	-
		$\dot{m}_g$	kg/s	31.66	-	31.66	-	[8]
		α_g	deg	69.28	-	-	-	-
	SAS	$T_{t,c,in}$	K	690.3	738.5	690.3	738.5	[8]
		$p_{t,c,in}$	bar	7.11	17.08	7.11	17.08	[8]
		SF	-	1.23		1.23		[6]

Table 7: (continued)

Component		Parameter	Unit	PrEDiCT		Literature		Source
				ADP	CDP	ADP	CDP	
R2	Inlet	$T_{t,g}$	K	1152.4	1196.0	-	-	-
		$T_{t,g,abs}$	K	1276.4	1324.7	-	-	-
		$p_{t,g}$	bar	3.65	8.62	-	-	-
		$p_{t,g,abs}$	bar	5.63	13.29	-	-	-
		$\dot{m}_g$	kg/s	31.66	-	31.66	-	[8]
		α_g	deg	25.19	-	-	-	-
	Outlet	$T_{t,g}$	K	1148.3	1191.8	-	-	-
		$T_{t,g,abs}$	K	1082.4	1123.3	-	-	-
		$p_{t,g}$	bar	3.56	8.41	-	-	-
		$p_{t,g,abs}$	bar	2.78	6.57	2.78	-	[6, p. 5]
		$\dot{m}_g$	kg/s	32.22	-	32.22	-	[8]
		α_g	deg	-55.82	-	-	-	-
	SAS	$T_{t,c,in}$	K	797.0	844.0	797.0	844.0	[8]
		$p_{t,c,in}$	bar	7.11	17.08	7.11	17.08	[8]
		SF	-	2.32		2.32		[6]
Stage 1		Ψ	-	1.43	-	1.48	-	[6, p. 5]
		ϕ	-	0.50	-	-	-	-
		Π	-	2.25	-	2.25	-	[6, p. 5]
		R	-	0.34	-	0.34	-	[6, p. 10]
		AN2	-	1.29	-	-	-	-
		Work Fraction	-	0.565	-	0.565	-	[6, p. 6]
		N. Stator Blades	-	46		46		[6, p. 12]
		N. Rotor Blades	-	76		76		[6, p. 12]
		Stator Solidity	-	0.74		0.71		[6, p. 12]
		Rotor Solidity	-	1.02		0.96		[6, p. 12]
		η_{Ts}	-	0.911[4]	-	-	-	-
Stage 2		Ψ	-	1.09	-	1.12	-	[6, p. 5]
		ϕ	-	0.53	-	-	-	-
		Π	-	2.11	-	2.11	-	[6, p. 5]
		R	-	0.33	-	0.33	-	[6, p. 10]
		AN2	-	2.32	-	-	-	-
		Work Fraction	-	0.435	-	0.435	-	[6, p. 6]
		N. Stator Blades	-	48		48		[6, p. 12]
		N. Rotor Blades	-	70		70		[6, p. 12]
		Stator Solidity	-	1.08		1.07		[6, p. 12]
		Rotor Solidity	-	1.01		1.06		[6, p. 12]
		η_{Ts}	-	0.907[4]	-	-	-	-
Spool 1		P	MW	16.03	-	16.03	-	[8]
		N	1/s	210.77	-	210.77	-	[8]
		$\dot{m}_f$	kg/s	0.65	-	0.65	-	[8]
		η_{Ts}	-	0.901[4]	-	0.924[4]	-	[6, p. 5]

[4]Defined in PrEDiCT according to [20, p. 670]. Using an alternative equivalent single blade approach for this spool results in an isentropic efficiency of 0.922. Definition for cooled turbine isentropic efficiency is unclear from literature data.

Copyright ©2024 Francisco Carvalho, Patrick Wehrel, Clemens Grunwitz, Robin Schöffler, Robin G. Brakmann This is an open access article distributed under the terms of the Creative Commons Attribution License, which allows reusers to distribute, remix, adapt, and build upon the material in any medium or format, so long as attribution is given to the creator. The license allows for commercial use.